KSCE Journal of Civil Engineering (2020) 24(8):2546-2559
DOI 10.1007/s12205-020-0168-1

pISSN 1226-7988, eISSN 1976-3808
www.springer.com/12205

Water Resources and Hydrologic Engineering

Groundwater Potential Mapping Using SWAT and GIS-Based Multi-Criteria Decision Analysis

Bisrat Ayalew Yifru[a,c], **Dereje Birhanu Mitiku**[b], **Mesfin Benti Tolera**[b], **Sun Woo Chang**[a,d], and **Il-Moon Chung**[a,d]

[a]*Civil and Environmental Engineering Department, University of Science and Technology, Daejeon 34113, Korea*
[b]*School of Civil Engineering and Architecture, Adama Science and Technology University, Adama 1888, Ethiopia*
[c]*Dept. of Land, Water and Environment Research, Korea Institute of Civil Engineering and Building Technology, Goyang 10223, Korea*
[d]*Member, Dept. of Land, Water and Environment Research, Korea Institute of Civil Engineering and Building Technology, Goyang 10223, Korea*

ARTICLE HISTORY

Received 30 January 2020
Accepted 22 April 2020
Published Online 30 June 2020

KEYWORDS

Groundwater potential
MCDA
Main Ethiopian Rift
Recharge
SWAT
SWAT-CUP

ABSTRACT

In several parts of the world, groundwater potential information gap limits the development and management of the resource. GIS-based multi-criteria decision analysis (MCDA) plays an important role in this regard. This work presents the groundwater potential mapping in a data-scarce region of Main Ethiopian Rift (MER) using Soil and Water Assessment Tool (SWAT) and GIS-based MCDA. SWAT was used to model the spatiotemporal variation of groundwater recharge. The calibration and validation results show the applicability of the model in the study area. The estimated monthly average recharge varies from 2.78 – 164 mm. The recharge, geomorphology, lithology, soil, land use/land-cover, and DEM derived topographic characteristics were analyzed using GIS-based MCDA to evaluate the groundwater potential. The result is classified into low, moderate, and high zones and validated using the wells and springs information available in the region. More than 61% of the area has moderate groundwater potential and less than 22% of the area has high groundwater potential.

1. Introduction

In arid and semi-arid areas, groundwater is the most valuable freshwater resource that can be developed fairly economical and used for agricultural, domestic, and industrial purposes (Calow et al., 2010). Its relative inherent important qualities such as drought reliability, low vulnerability, free of chemical and biological contaminants, and abundance, with good management practice, make groundwater the most dependable water resource all over the world (Jha et al., 2007). In rural areas, groundwater consumption is increasing from time to time while the management practice is traditional (Andualem and Demeke, 2019; Das, 2019). Several parts of the world follow the costly and time consuming traditional hydrogeological studies (usually drilling) and the input towards groundwater resources management is limited (Berehanu et al., 2017; Hussein et al., 2017; McCormack et al., 2017). Surface water and groundwater models are important tools to explore and understand the features and status of a watershed in most possible details (Li et al., 2018) though watershed-scale models have an extensive data requirement for calibration and validation purposes.

The movement of groundwater depends on hydrological, lithological, atmospheric, soil, and topographic nature of a region (Andualem and Demeke, 2019; Das, 2019; Mallick et al., 2019) and therefore, the groundwater study needs multidisciplinary data. GIS-techniques play a vital role in processing, understanding, organizing, and quantifying a vast number of data with minimal error (Jha et al., 2007). Recently, GIS-based multi-criteria decision analysis (MCDA) has been employed in various places to map groundwater potential zone (GWPZ) (Arulbalaji et al., 2019; Mallick et al., 2019), including watersheds in Ethiopia (Bashe, 2017; Hussein et al., 2017; Andualem and Demeke, 2019). GWPZ mapping using GIS techniques and MCDA has several advantages over traditional studies including the ability to define hydrological and hydrogeological features of a study area in the spatial context (Nair et al., 2017).

CORRESPONDENCE Il-Moon Chung imchung@kict.re.kr Civil and Environmental Engineering Department, University of Science and Technology, Daejeon 34113, Korea; Dept. of Land, Water and Environment Research, Korea Institute of Civil Engineering and Building Technology, Goyang 10223, Korea

However, the previous studies were focused mainly on the lithology and topographic attributes and rainfall distribution of the study area (Bashe, 2017; Nair et al., 2017; Arulbalaji et al., 2019; Mallick et al., 2019). A detailed review of the application of GIS-based MCDA in GWPZ mapping and the thematic layers used are tabulated by Mallick et al. (2019); no study included groundwater recharge in GWPZ mapping.

Rainfall distribution may not represent the groundwater recharge distribution as recharge is affected by different factors including soil type, geology, slope, and land cover (Rashid et al., 2012; Ibrahim-Bathis and Ahmed, 2016; Mallick et al., 2019). Especially in a region with a complex topographic nature such as Ethiopian watersheds considering rainfall distribution as the main factor in the groundwater potential mapping may result in misleading conclusions. In a data-scarce region, understanding the spatiotemporal distribution of the recharge in addition to the GWPZ adds significant value to the sustainable management of the resource.

Numerous watersheds in Ethiopia fall under the category of low hydrological measurement, not well documented geomorphological characteristics, and limited investigation of hydrogeological features (Ayenew et al., 2008a, 2008b; Berhanu et al., 2013; Berehanu et al., 2017; Tegegne et al., 2017; Aga et al., 2018). As a result, the groundwater potential is left uninvestigated in socio-economically important regions of the country (Ayenew, 2007; Halcrow and GIRDC, 2008; Izady et al., 2014); the development and abstraction are based on several decades-old studies. Nevertheless, due to the relative cost, the complexity of management, limitation, and evaporation loss of surface water, the water supply is primarily reliant on the groundwater.

Main Ethiopian Rift (MER) is an important area in the country in connection with its water resources (Legesse and Ayenew, 2006; Pascual-Ferrer et al., 2014; Berehanu et al., 2017; Desta and Lemma, 2017). In MER, there are a few machines-drilled boreholes, but most of them are controversial due to their low productivity and some of them are drying. As the water supply-demand increases the potential for future development and abundant use of the groundwater resources is an important issue to deal with (Izady et al., 2014; Mechal et al., 2017).

In this study, to map the GWPZ in a data-scarce region of MER (Katar watershed), we have proposed a new procedure, which is a combination of Soil and Water Assessment Tool (SWAT) and GIS-based MCDA. The recharge is estimated using SWAT and then incorporated into the GIS-based MCDA together with geomorphology, lithology, soil, land use/land-cover (LULC), and DEM derived topographic characteristics. The spatiotemporal distribution of groundwater recharge is also presented from the calibrated and validated SWAT model.

In Katar watershed, there are around 21 small towns. Most of the towns are classified as, by the Ministry of Water Resources, Irrigation, and Electricity (MoWIE), most critical water supply towns (Halcrow and GIRDC, 2008). Related to groundwater resources the Katar watershed is one of the unexplored watersheds in MER due to mainly the limited information available, in addition to the common problem of intricate geological and hydrogeological nature of the region. As stated in the groundwater study report of MER by Halcrow and GIRDC (2008), the limited studies and the available data in this watershed are contradicting with the hydrogeological systems described in the master plan study of the country. Therefore, the procedures and conclusions from this work provide base information for policymakers, future investigation of groundwater resources in the watershed and other watersheds, which have similar nature with the current study area. It will be also a useful input for the community and non-governmental organizations in their groundwater development work.

2. Materials and Methods

2.1 Study Area

The Ethiopian rift is predominantly covered with volcanic and sedimentary rocks which are the result of sedimentary and volcano-tectonic processes (Ayenew, 2007). It is a region with tectonically active complex hydrogeological and discontinuous aquifers disrupted by faults founding the rift resulted in variable groundwater occurrence, discharge, depth, and flow patterns (Legesse and Ayenew, 2006; Kebede et al., 2008; Kebede, 2013; Mechal et al., 2016, 2017).

The study area is one of the watersheds in MER called Katar watershed (Eastern Lake Ziway). Katar watershed has a coverage area of around 3,580 square kilometers. Katar River and its tributaries drain from Southeast highlands to the Northwest and join Lake Ziway. Lake Ziway and Chilalo, Kaka, and Tulu Moye Mountains are locally known natural landmarks that surround the watershed. Topographically, Katar watershed shows a well pronounced varies with the altitude ranging from around 1,612 m above sea level near Lake Ziway to about 4,213 m above sea level on the high volcanic ridges along the East of the watershed. The highlands are mainly rain-fed agricultural areas.

Katar watershed has instrumented with weather and streamflow measurements. The river is gauged at Abura, around Ziway Lake (Fig. 1). Countrywide geology, soil property, and LULC data are available as well.

2.2 Recharge Estimation and Groundwater Potential Mapping

The hydrological simulation was performed using the SWAT and GIS-based MCDA was employed to map the GWPZ. In the GWPZ mapping process 12 important groundwater affecting variables specifically soil, lithology, geomorphology, LULC, topographic characteristics derived from DEM viz slope, drainage density, lineament density, curvature, topographic wetness index (TWI), roughness, topographic position index (TPI), and recharge from SWAT output were analyzed.

Brief description and setup processes of the SWAT model, GIS-techniques, and MCDA are given here; the details are presented by (Abbaspour et al., 2007; Saaty, 1987, 2008; Arnold et al., 1998, 2012). The method followed to map the groundwater

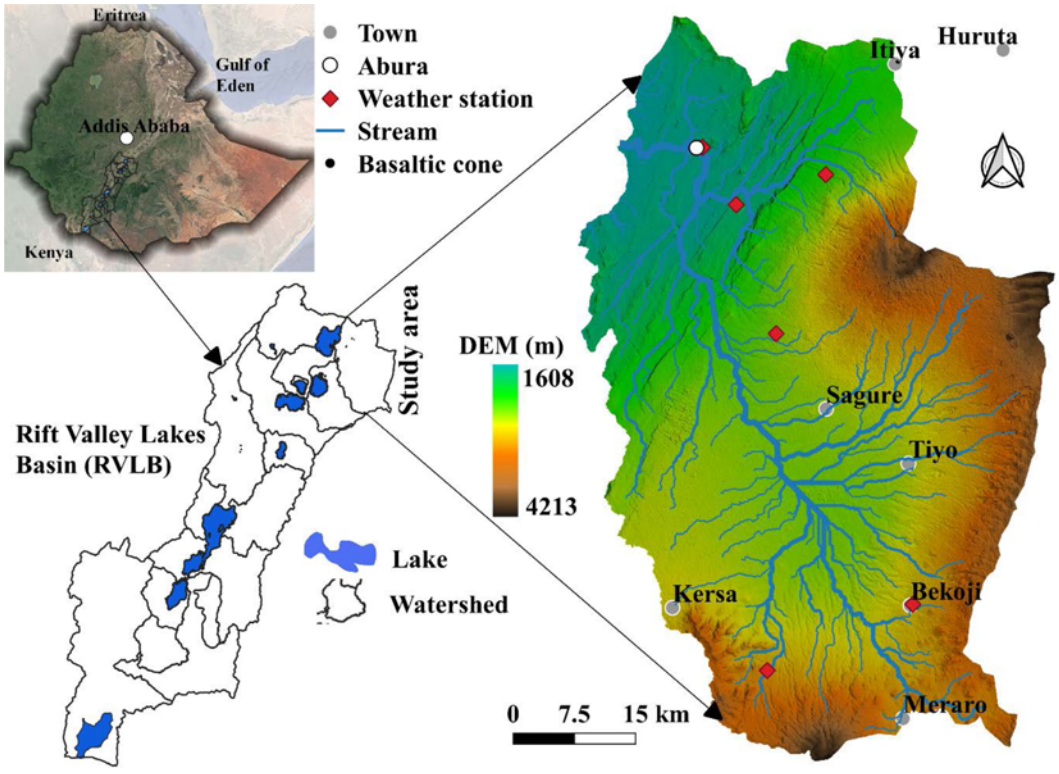

Fig. 1. Location Map — Meteorological Stations, Stream Network and Order, and Topography of Katar Watershed

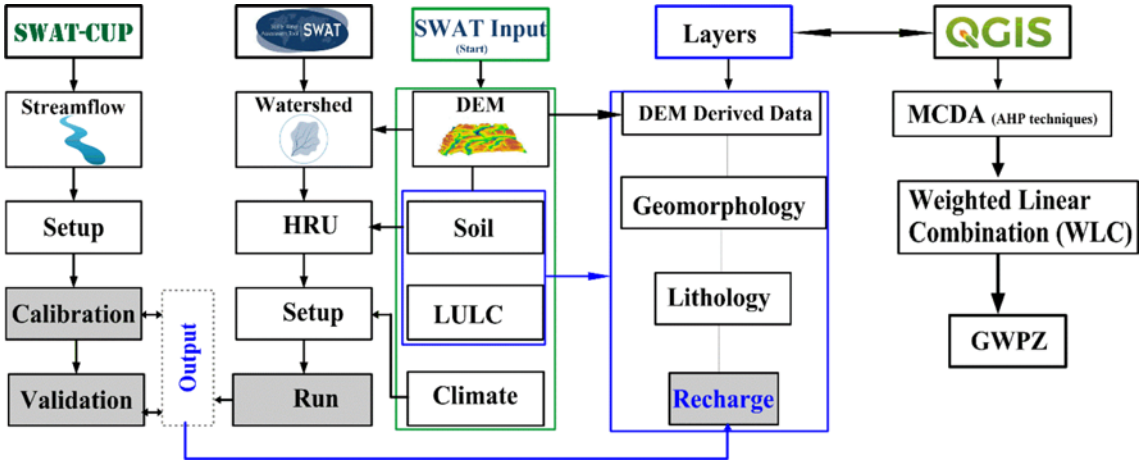

Fig. 2. The Framework of the Methods Followed in This Study including SWAT Model Development and Calibration Process (HRU is hydrologic response units.)

potential is depicted in Fig. 2; the detailed data processing, setup processes, and GIS works are excluded to be discussed in later sections.

2.2.1 Recharge Estimation

The recharge is the primary way through which water joins the aquifer and thus quantifying it is vital for integrated, sustainable management, and use of groundwater and surface water resources (Githui et al., 2012; Jin et al., 2015). SWAT model has been applied to estimate recharge (water balance in general) all over the world (Awan and Ismaeel, 2014; Githui et al., 2012; Jin et al., 2015; Eshtawi et al., 2016; Putthividhya and Laonamsai, 2017).

SWAT is a physically-based hydrologic/water quality, and hydrologic response units (HRU) based large area watershed model (Abbaspour et al., 2007; Arnold et al., 2012). SWAT uses spatiotemporal data to simulate water flow in soil and groundwater, erosion, nutrient cycling, and others (Arnold et al., 1998). There are different versions of SWAT with different interfaces; here version 2012 with QGIS interface (QSWAT) was employed.

HRU is the smallest segment of a watershed representing a diverse LULC, soil, and landscape characteristics within the subbasins. Flow is calculated for each segment of the watershed

separately. The general equation of the SWAT model is the following (Arnold et al., 1998):

$$SW_t = SW_0 + \sum_{i=1}^{t}(R_{day} - Q_{surf} - ET - W_{perc} - Q_{gw}) \quad (1)$$

where SW_0 and SW_t are the quantity of initial and final soil water (mm/day); t is the time (days); R_{day} is the precipitation (mm/day); Q_{surf} is the surface runoff (mm/day); ET is the evapotranspiration (mm/day); W_{perc} is the percolation (mm/day); Q_{gw} is the flow from the aquifer (mm/day).

SWAT simulates two aquifers for individual subbasin: a shallow unconfined aquifer that donates water to the main stream or reaches of the subbasin and a confined deep aquifer (Arnold et al., 1993). The total recharge is computed using the following equation:

$$W_{rch,i} = \left(1 - e^{-\frac{1}{\delta_{gw}}}\right) w_{seep} + e^{-\frac{1}{\delta_{gw}}} W_{rch,i-1} \quad (2)$$

where $W_{rch,i}$ and $W_{rch,i\text{-}1}$ are water inflowing to the aquifer on day i and day i-1, δ_{gw} the drainage delay time of the top formation (days), and W_{seep} is the water leaving from the soil profile at the bottom (day i) which can be calculated using the following relationship:

$$W_{seep} = W_{perc} + W_{crk,btm} \quad (3)$$

where W_{perc} is the water escaping from the second layer (mm/day), and $W_{crk,btm}$ is the bypass flow from the soil profile at the lower boundary (day i).

The deep aquifer obtains some portion of the total recharge approximated with the following formula:

$$W_{deep} = \beta_{deep} \times W_{rch} \quad (4)$$

where W_{deep} is the water moving from shallow to the deep aquifer (day i), β_{deep} is the percolation coefficient, and W_{rch} is as defined in Eq. (2).

2.2.2 Multi-Criteria Decision Analysis

GIS-techniques and MCDA are effective tools for storing, processing, evaluating, and ranking alternatives in the water resources management sector (Tkach and Simonovic, 1997). analytical hierarchical process (AHP) is a widely used MCDA technique based on the concept of driving ratio scales from the paired comparison (Saaty, 1987) and it is known to be an easy solution for complex decisions (Podvezko, 2009). Studies show that it has superior accuracy in groundwater potential mapping compared to other methods such as the Catastrophe technique (Singh et al., 2018).

In this work, a GIS-based AHP is used to integrate thematic layers, which influence the natural storage and movement of water. Since the pairwise comparison is vital in the AHP application, the association of layers is weighted according to their contribution to groundwater existence based on Saaty's parameter scaling. Saaty's parameter scaling varies from one to nine: "1 – equal importance, 2 – equal to moderate importance, 3 – moderate importance, 4 – moderate to strong importance, 5 – strong importance, 6 – strong to very strong importance, 7 – very strong importance, 8 – very to extremely strong importance, and 9 – extreme importance" (Saaty, 1987).

Therefore, in this GWPZ mapping process, the ranking was done twice. First, each thematic layer of internal attributes was ranked and recoded. Second, all the layers compared and the rank was given based on their influence on groundwater availability. The data processing and ranking were done with the help of a literature survey (Berhanu et al., 2013; Bashe, 2017; Hussein et al., 2017; Mallick et al., 2019), experience, and an acquaintance of the area. Then the matrix of all thematic layers with the assigned weight was constructed.

Consistency—a measurement of dependency within and between the sets of thematic layers of its structure—is important in AHP (Saaty, 1987). The consistency ratio (CR), principal Eigenvalue (λ_{max}), and consistency index (CI) were calculated using the following Saaty's CI equations:

$$CI = \frac{\lambda_{max} - n}{n - 1} \quad (5)$$

$$CR = \frac{CI}{RCI} \quad (6)$$

where n is the number of data considered and RCI is random consistency index value (Podvezko, 2009).

A CR of 10% or less is satisfactory to proceed with the analysis (Saaty, 1990). However, if the consistency index exceeds 10%, reconsidering the judgment is necessary to identify the sources of inconsistency and adjust it accordingly. A zero value of CR indicates that the pairwise comparison has a perfect consistency.

The normalized weight of all the data was produced from the pairwise comparison matrix and the GWPZ map was produced using weighted linear combination (WLC) technique. WLC is founded on the theory of a weighted averaging where the criteria are standardized to the same numeric bound (Drobne and Lisec, 2009). The method can be applied using the GIS; it is simple and it can be equated as follows:

$$GWPZ = \sum_{i=1}^{n}(Weight_i \times Thematic\ Layer_i) \quad (7)$$

2.2.3 Calibration and Validation

The SWAT simulation was performed for 21 years (1990 – 2010) including two years of warmup period. The calibration was performed for the first 11 years after the warmup period and the remaining data were used to validate the model. Streamflow data recorded at the Abura gauging station were used to calibrate and validate the SWAT model.

The calibration and validation were performed using semi-automated SUFI-2 (sequential uncertainty fitting version 2) in SWAT-CUP in monthly time steps. Using global sensitivity analysis method in SUFI-2 algorithm, twelve most sensitive parameters were selected namely soil water (SOL_K, SOL_BD, and SOL-AWC), groundwater (GW_DELSY, ALPHA_BF, GWQMN, and GW_REVAP), lateral flow (HRU_SLP), surface

Table 1. Flow Parameters Definition and Ranges Selected for Calibration

Parameter	Definition	Range
r__CN2.mgt	Runoff curve number by Soil Conservation Service(SCS)	-0.5 – 0.5
v__GW_DELAY.gw	Groundwater delay (days)	0 – 500
v__GWQMN.gw	Minimum depth of water required in the shallow aquifer for return flow to be initiated (mm H_2O)	0 – 5000
v__GW_REVAP.gw	A coefficient that shows how ready the water to moves to the root zone from the shallow aquifer	0.02 – 0.4
v__ALPHA_BF.gw	Baseflow recession coefficient	0 – 1
v__ESCO.hru	A coefficient to adjust the soil evaporation demand	0 – 1
v__CH_K2.rte	Hydraulic conductivity of the main channel (mm/hr)	0.01 – 150
r__SOL_AWC.sol	Soil available water capacity (mm H_2O/mm soil)	-0.5 – 0.5
r__SOL_K.sol	Saturated hydraulic conductivity (mm/hr)	-0.5 – 0.5
v__SURLAG.bsn	Coefficient of surface runoff lag	0.05 – 24
r__HRU_SLP.hru	Average slope steepness (m/m)	0 – 0.6
r__SOL_BD.sol	Moist bulk density (Mg/m^3)	-0.5 – 0.6

Note: v__parameter value is replaced; r__parameter value is multiplied by (1+ a given value)

runoff (SURLAG and CN2), evaporation (ESCO), and main channel hydraulic conductivity (CH_K2) and modified by comparing modeled and measured flow data. The definition and minimum-maximum values fixed in the calibration are tabulated (Table 1).

The calibration and validation performance was evaluated using four commonly used indicators: coefficient of determination (R^2), Nash–Sutcliffe coefficient of efficiency (*NSE*), percentage bias (*PBIAS*), and *RSR* (standardize root mean square error) (Moriasi et al., 2007).

The concept behind R^2 is common and simple; it tells whether the observed and computed data have a linear association. The value normally varies from 0 – 1; the closer to one the better fitted.

$$R^2 = \left\{ \frac{\sum_{i=1}^{n}(Q_i-\overline{Q})(S_i-\overline{S})}{[\sum_{i=1}^{n}(Q_i-Q)^2]^{0.5}[\sum_{i=1}^{n}(S_i-\overline{S})^2]^{0.5}} \right\}^2 \quad (8)$$

NSE has a nearly similar concept with the coefficient of determination; it is a normalized value that shows the relative size of the residual and observed data variance. It indicates how fit is the observed and computed flow in the 1:1 line plot. The values of *NSE* ranged from -∞ – 1. The closer to one the better the performance of the model but to accept the result the *NSE* greater than 0.5 is indorsed (Moriasi et al., 2007). *NSE* set as the objective function in both the calibration and validation process.

$$NSE = 1 - \frac{\sum_{i=1}^{n}(Q_i-S_i)^2}{\sum_{i=1}^{n}(Q_i-\overline{Q})^2} \quad (9)$$

RSR is a simple statistical parameter, which calculates the standard deviation of model prediction error. The recommended value is 0.0 – 0.7; zero is very good and 0.7 just satisfactory.

$$RSR = \frac{\sqrt{\sum_{i=1}^{n}(Q_i-S_i)^2}}{\sqrt{\sum_{i=1}^{n}(Q_i-\overline{S}_i)}} \quad (10)$$

PBIAS shows the propensity of the calculated discharge to be higher or lower than the observed discharge. While the recommend value varies from -25 – 25 as the value of *PBIAS* gets closer to 0.0 the accuracy of the model increases, positive value implies underestimation and negative value overestimation (Moriasi et al., 2007; Rouholahnejad et al., 2012).

$$PBIAS = \left[\frac{\sum_{i=1}^{n}(Q_i-S_i)\times(100)}{\sum_{i=1}^{n}(Q_i)} \right] \quad (11)$$

In Eqs. (8) – (11), Q_i and S_i are the observed modeled discharge for the i^{th} day of modeling period; $\overline{Q}$ and $\overline{S}$ are mean of *n* observed and calculated discharge respectively.

The GWPZ map was validated by mapping the selected springs and wells in the area. In the region, most of the wells are located in the lower area around Ziway Lake and springs are located even in the hilly area. However, the information is limited due to that most of the wells are private wells and the springs information is not well recorded. The GWPZ map was validated using groundwater pumping wells and springs data. The pumping capacity and springs yield in the region vary from 2.6 – 1,036 m^3/day. Most of the wells are shallow wells; the static water level is less than 80 m except one well that has a 245 m. For this study, 15 boreholes and springs were selected based on their recorded production rate and location.

2.3 Data Sources and Processing

Both the SWAT model and the GWPZ mapping have extensive data requirements. The SWAT model needs time-series and spatial data including solar radiation, rainfall, wind speed, temperature, and relative humidity. We have collected the data mainly from different offices and freely available websites as described in Table 2.

Geomorphology, lithology, streamflow, soil, and springs and wells data were obtained from the MoWIE database. A 30 m spatial resolution LULC and DEM were downloaded from GlobeLand30 (Jun et al., 2014) and USGS, respectively. The

Table 2. Raw and Processed Data Sources and Descriptions

Data (Raw data)	Source and description
Climate	National Meteorological Service Agency of Ethiopia
Streamflow	Ministry of Water Resources, Irrigation, and Electricity, Ethiopia
LULC	GLOBELAND 30 (Jun et al., 2014)
Soil	Harmonized world soil database (FAO)
DEM	USGS "earthexplorer" website
Lithology Geomorphology Spring and well	Ethiopian Ministry of Water Resources, Irrigation, and Electricity
Recharge	Processed from SWAT model output
DEM derived data	These maps are processed using different algorithms in GIS, the maps are Lineament density, Slope, Roughness, TPI, TWI, Curvature, and Drainage density

DEM-derived topographic attributes were processed mainly using SAGA in the QGIS interface. All the maps were re-projected to Adindan/UTM zone 37N before incorporating in the modeling and GWPZ mapping process.

2.3.1 SWAT Model Inputs and Setup Process

The major SWAT model inputs are DEM, soil, LULC, and weather data. The model setup starts with importing grid-based spatial data, delineating the watershed, creating subbasins, and definition of HRU. The SWAT model uses DEM to delineate the watershed and create stream networks and subbasins. The watershed was divided into 47 subbasins and the subbasins into 1651 HRUs; each HRU has unique LULC and soil property.

LULC influences both surface water and groundwater — the effect is mainly reflected in the recharge change (Lerner and Harris, 2009). Katar watershed has eight land-cover classes as shown in Fig. 3(a); more than 80% of the area coverage is agricultural.

Figure 3(b) shows the soil attributes used in the model. The classification shows four major soil groups specifically CM – Cambisols, LP – Leptosols, LV – Luvisols, and VR – Vertisols. The dominant soil is clay in the area.

To complete the SWAT model setup the climate data were processed using weather generator model WXGEN, prepared in the required format, and added to the SWAT model database. Six weather station data were processed and imported into the model.

2.3.2 Lithology and Geomorphology

The occurrence and flow of groundwater in MER is controlled mainly by Lithology and geomorphology of the region (Bashe, 2017; Halcrow and GIRDC, 2008; Mechal et al., 2016). Lithology determines the water movement, storage, and quality. Geomorphology represents the landform and is one of the key elements used commonly to map the GWPZ (Hussein et al., 2017).

Even though the geomorphology of Katar watershed can be grouped into two large groups as alluvial and volcanic landforms, it has intricate features consisting of a complex of volcanic cones, low to high mountainous reliefs, plains, steep slopes, and seasonal swamps and marshes. Fig. 4(a) shows the different geomorphological zones. Interestingly, more than 60% of the area is covered by four of the formations, namely Ssv, Av1, Vp1, and Vx1. Ssv stands for fault plain and low plateau complexes with several fault scarps, sags, cones, vents, and crater remnants and it is the biggest by covering around 20% of the area. AV1 consists of majorly lacustrine plains; Vp1is surging plateau formed primarily on pyroclastic deposits. Vx1 is volcanic forms of steep severely dissected side slopes, small volcanic vents, and cone remnants.

The rest of the area is characterized as large degraded volcanoes and volcanic complexes of dramatic mountainous relief (Vz3) along the Chilalo Mountain. Around Ziway Lake, the watershed

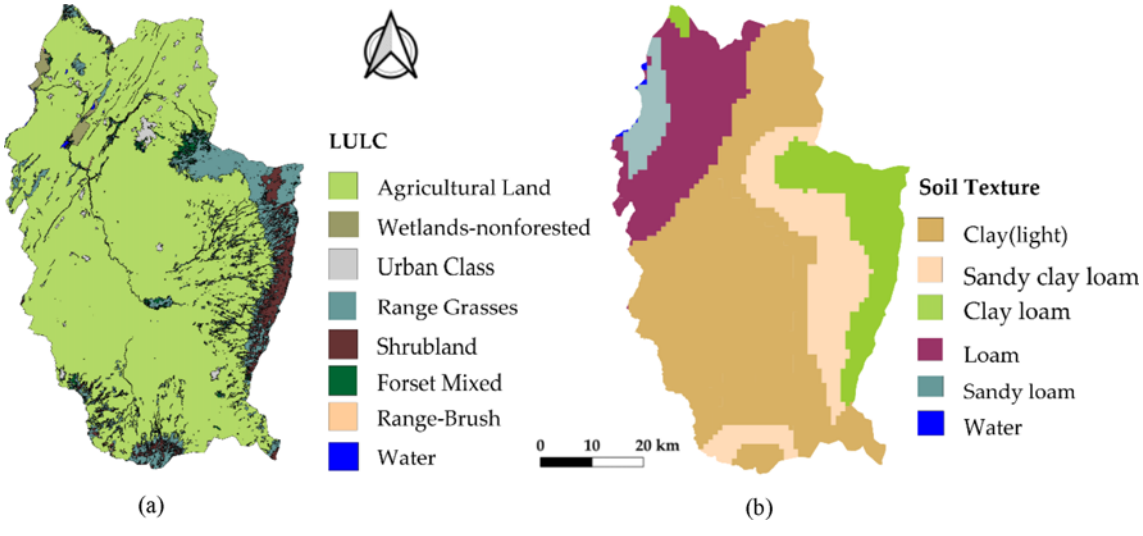

Fig. 3. LULC and Soil Classes: (a) LULC, (b) Soil Texture

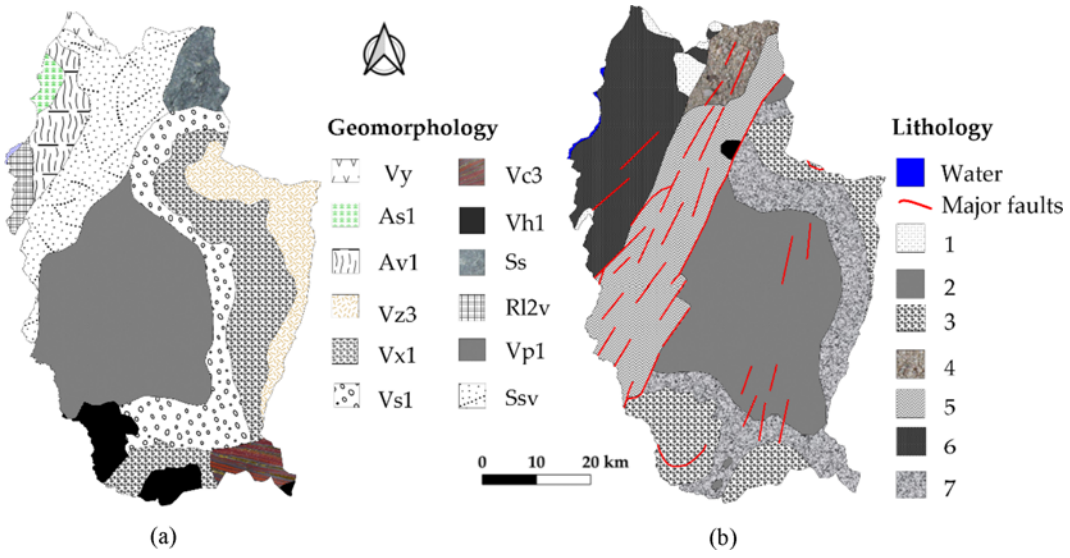

Fig. 4. Geomorphological and Lithological Zones: (a) Geomorphology, (b) Lithology

is covered dominantly by piedmonts of extinct central volcanoes, parasitic cone, and vent remnants—represented by (Vs1) in the figure, low to moderate relief hills (Rl2v), and seasonal swamps and marshes (As1). Moreover, mountainous relief hills (Vh1), high mountain stone (Ss), complexes of plugs, vents, craters, volcanic cones, piedmont plains, and other volcanic remnants—grouped as Vc3, young volcanoes, and related volcanic forms of high mountainous relief—grouped and represented by (Vy) are the characteristics of the Northern and Southern part of the watershed.

The major aquifers in the rift system are fractured inter-layered basalts and ignimbrites (Japan International Cooperation (JICA), 2012). The shallow groundwater aquifers are principally young quaternary basalts (Kebede et al., 2008). As depicted in Fig. 4(b), the watershed is characterized by seven major lithological groups and summarized as follows:

1. Rhyolitic volcanic centers, pumice, obsidian pitchstone, tuff, subordinate trachytic flows, ignimbrite
2. Nazret series: ash flows, ignimbrites, rhyolitic flows, unwelded tuffs, domes and trachyte
3. Alkaline basalt
4. Spatter cones, basalt flows, and hyaloclastite
5. Dino formation including coarse pumice, ignimbrite, tuff, and water-lain pyroclastic rocks
6. Lacustrine and alluvial and deposits: clay, sand, limestone, silt, diatomite, and beach sand
7. Trachy-basalt, trachyte, peralkaline rhyolite with subordinate alkaline basalt

Dominantly the area is covered by pumice, rhyolitic volcanic centers, obsidian pitchstone, ignimbrite, tuff, subordinate trachytic flows, and other formations. Associated with depression and plateau several major fault lines cross the MER in the Northeast and Northwest direction and have the potential of facilitating the storage and transmission of groundwater; surface water losses to the faulted system and provide extensive areas of recharge in many watersheds such as Katar watershed (Halcrow and GIRDC, 2008).

2.3.3 DEM-Derived Topographic Attributes

Important topographic attributes that determine the hydrological characteristics of a watershed can be derived from DEM (Wu et al., 2008). In this work, TWI, TPI, curvature, slope, lineament density, drainage density, and roughness were derived from a 30 m resolution DEM. The layers are presented in Figs. 5 – 7. Because of the topographic complexity, most of the layers show the complex distribution of classes and found difficult to produce easy to glimpse maps, however, the dominant classes of each map are easy to distinguish.

2.3.3.1 Drainage and Lineament Density

The drainage and lineament density of the watershed are presented in Fig. 5. Lineaments are naturally occurring curvilinear or linear structurally controlled features in a landscape, which are an expression of an underlying geological structure, including faults (Bashe, 2017; Nair et al., 2017). The lineament density is generated by extracting the lineament from the DEM using the Geomatica toolbox and the drainage network is created using QGIS.

These two maps of density of lines (Fig. 5) play a vital role in the groundwater system as an enhanced natural recharge way and as an outlet of the aquifer. The groundwater potential increases as the lineament density increases (Rashid et al., 2012), whereas drainage density and infiltration capacity of the formations have an inverse relationship (Nair et al., 2017). Accordingly, the drainage and lineament density of the area is assembled into five classes and the high weight represents low-drainage density classes.

2.3.3.2 Slope, Roughness, TPI, Curvature, and TWI

TWI quantifies how much the topography is favorable in facilitating

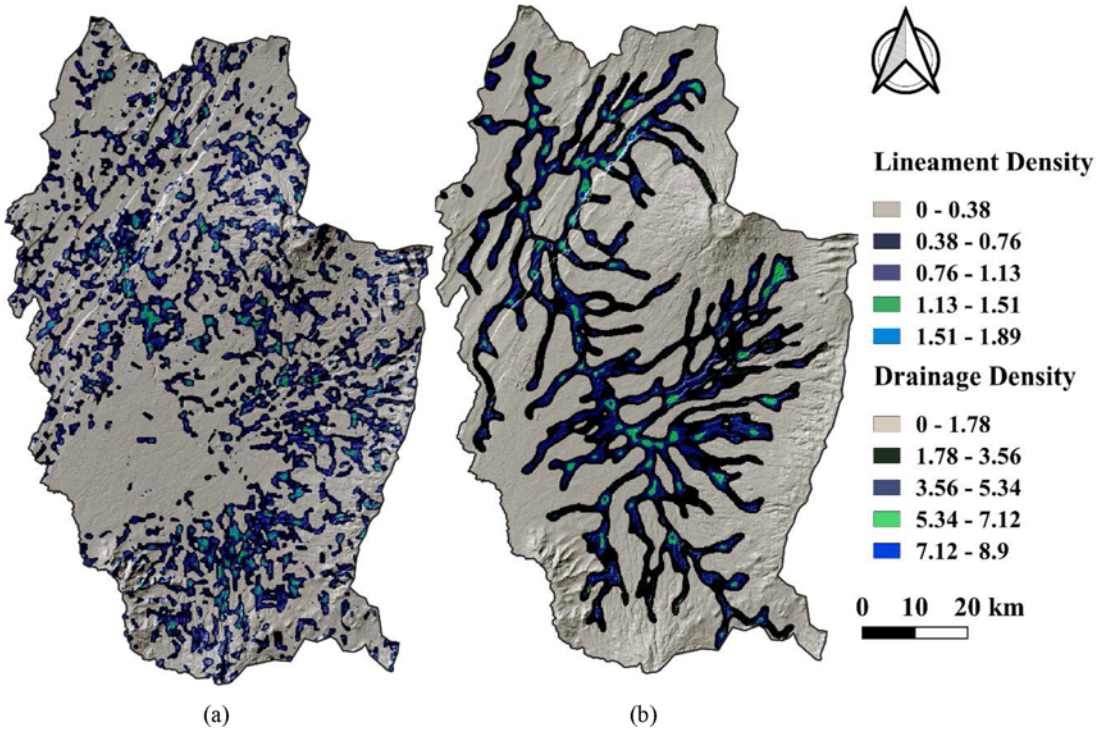

Fig. 5. Drainage and Lineament Density Classes (Km/Km^2): (a) Lineament Density, (b) Drainage Density

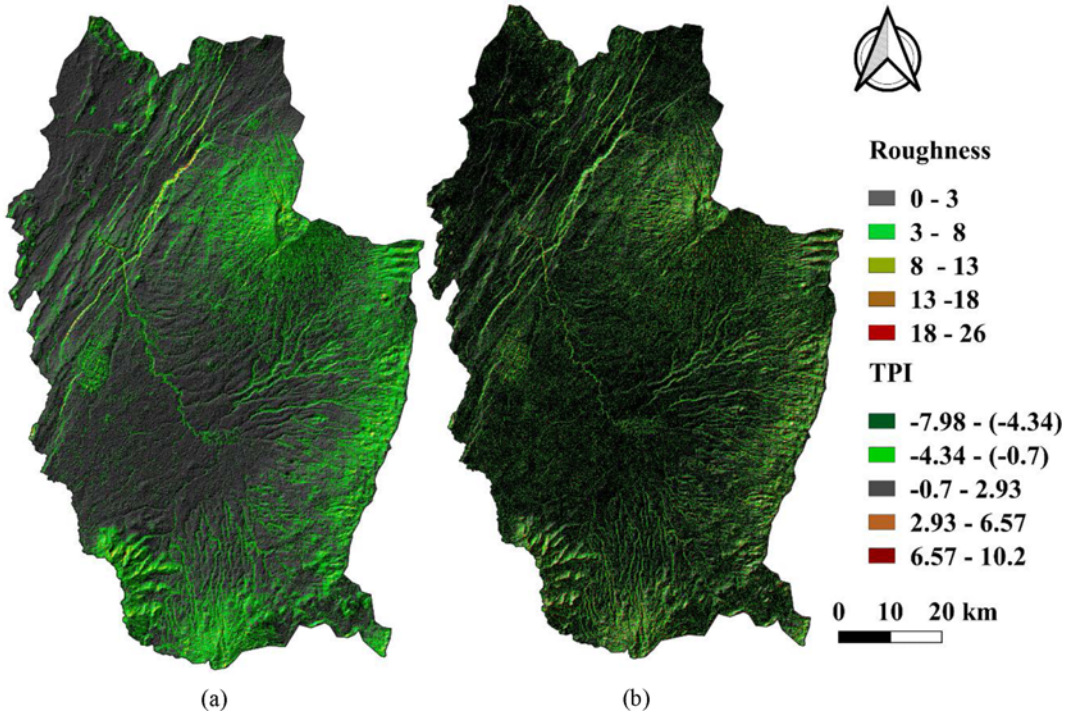

Fig. 6. Classes of Topographic Roughness and TPI: (a) Roughness, (b) TPI

the recharge process from precipitation; the others characterize the topographic undulation. Curvature and TWI have a direct relationship with the groundwater potential, whereas the rest of the parameters have an indirect relationship. Therefore, the weight of the class was assigned accordingly. The classes are presented in Figs. 6 – 7, except the slope.

The slope expresses the steepness. It is an expression of shape and relief of the ground surface. The runoff and infiltration rates are controlled fundamentally by the slope of the surface. On steep slope areas, the recharge is less compared to gentle slope

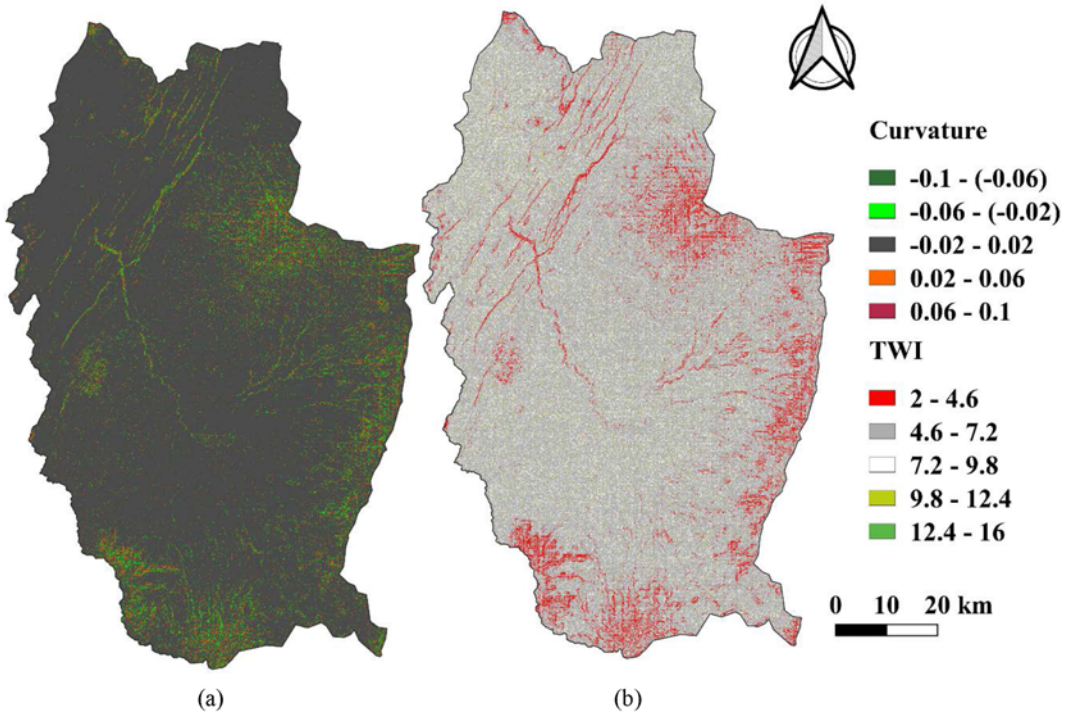

Fig. 7. Topographic Curvature and TWI: (a) Curvature, (b) TWI

areas (Manna et al., 2016). The slope of Katar watershed varies from 0.015 – 55 degrees and classified into "flat or almost flat (0 – 3), gently sloping (3 – 8), sloping (8 – 15), moderately steep (15 – 30), steep (30 – 50), and very steep (50 – 55)" based on (Berhanu et al., 2013) suggested classification.

Figure 6 shows the roughness and TPI. The roughness is mainly a characteristic of weathered rocks. It shows how big is the inter-cell difference of a central pixel from its surrounding cells in a DEM. An area rich with thick weathered rocks has a less GWPZ compared to a highly rough topography where usually a thin layer of weathered area dominates and hence less possibility for groundwater availability. High roughness means high undulation. Regions, which show high undulation, are generally mountainous where the landscape is suffered from continuous weathering and erosion processes (Nair et al., 2017). The roughness of the Katar watershed ranges from 0 – 26.

TPI shows the central pixel difference compared to the mean of its surrounding cells, the value can be negative or positive. When the central point is higher than the average surroundings, the value of TPI is positive (Weiss, 2001). TPI of Katar watershed varies from -7.98 – 10.2 and high groundwater potential weight was given for high negative TPI values.

Topography can be also characterized using its concavity and convexity nature (White, 1966) and it is commonly known by its quantitative expression — curvature. Curvature helps to tell whether a topography is concave upward or downward quantitatively. Water tends to decelerate and accumulate in convex profile and concavity has the opposite effect. A curvature range of the study area is -0.1 – 0.1 (Fig. 7).

TWI reflects the role of topography on hydrological processes: showing the ration of the upstream contributing area with an orthogonal breadth to the flow direction (Beven and Kirkby, 1979; Sørensen et al., 2006). TOPMODEL – an algorithm that simulates a watershed-scale flow of water – was employed to simulate TWI in QGIS. In the Katar watershed, the TWI varies from 2 – 16 but the majority of the area is covered with TWI value ranging from 4.6 – 7.2 and the mountainous region shows a low TWI value (Fig. 7).

3. Results

The outputs from SWAT namely streamflow, evapotranspiration (ET), surface runoff, and recharge and the GIS-based MCDA results – towards groundwater potential mapping – are presented in Figs. 8 – 11. The streamflow is presented as a comparison of modeled and observed flow at the Abura gaging station. Other SWAT results are an average of all the subbasins of Katar watershed. The statistical performance indicators in both the calibration and validation of SWAT and the thematic layers with the assigned ranks and final normalized weight are also tabulated.

3.1 SWAT Model Outputs

Figure 8 shows the comparison of measured and computed streamflow in a monthly time step over a period of 1992 – 2010. The two lines—measured and simulated streamflow – show reasonably similar peaks and lows except in the year of 1997 and 2002 and the immediately following year. The two years were drought years in the country; the flow changed suddenly from the normal flow of the preceding years to low flow and then back to the normal flow in the next year and as a result, the model

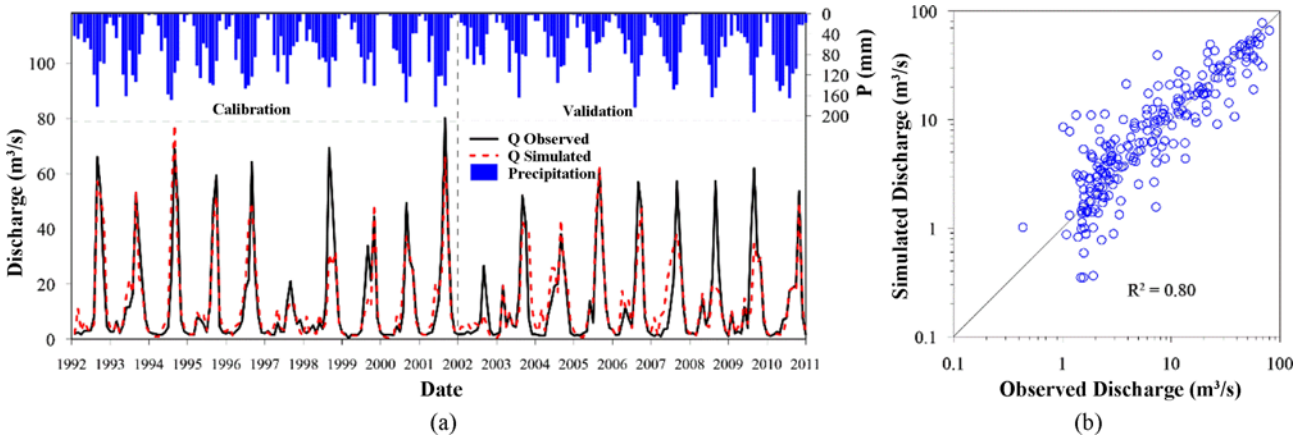

Fig. 8. Monthly Observed and Simulated Streamflow over a Period of 1992 — 2010: (a) Seasonal Variation, (b) Scatter Plot

could not capture the flow pattern compared to the other years in simulation period.

Besides the above-mentioned drought periods, the precipitation in the area was not regular due to the occurrence of long and short rainy seasons in the years of 1994, 2004, 2008, and 2010. The common wettest months in the country are from half of June – August but in the year 1994 and 2010 longer rainy season with a moderate peak was recorded. The precipitation record also shows high Autumn rain in the years 2004 and 2008. The cumulative effect of these precipitation irregularities is reflected in the peaks and lows of the discharge in the area as shown in the figure.

Despite the above-mentioned anomalies happened in these 19 years the observed and simulated streamflow pattern is fairly acceptable. In addition to the visual inspection of Fig. 8, the statistical model performance parameters support this inference.

Table 3 shows the model performance statics in the calibration validation period. All the tabulated parameters are in the recommended range (Moriasi et al., 2007). However, most parameters show lower performance value in the validation compared to the calibration period, such as NSE is 0.83 in the calibration lowered to 0.74 in the validation. The most likely reason is that the validation period started after the 2002 drought period in the area.

Table 3. Statistical Values of Calibration and Validation Performance

Parameter	Calibration	Validation
NSE	0.83	0.74
R^2	0.83	0.74
PBIAS	2.4	-1.2
RSR	0.41	0.51

Figures 9 and 10 show the spatiotemporal variation of recharge in Katar watershed. Fig. 9 depicts the average monthly recharge, surface runoff, and evapotranspiration (ET). The seasonality of the recharge and the principal water balance components can be seen clearly. From the overall period, the years 1997, 2002, and 2005 have the minimum recharge values.

From the statistical analysis, it was found that the maximum monthly average recharge is 27 mm and in December and January, the recharge is almost zero. Around 44% of the recharge occurs in Agust which counts around 21% of the areal precipitation in the watershed. More than 85% of the recharge

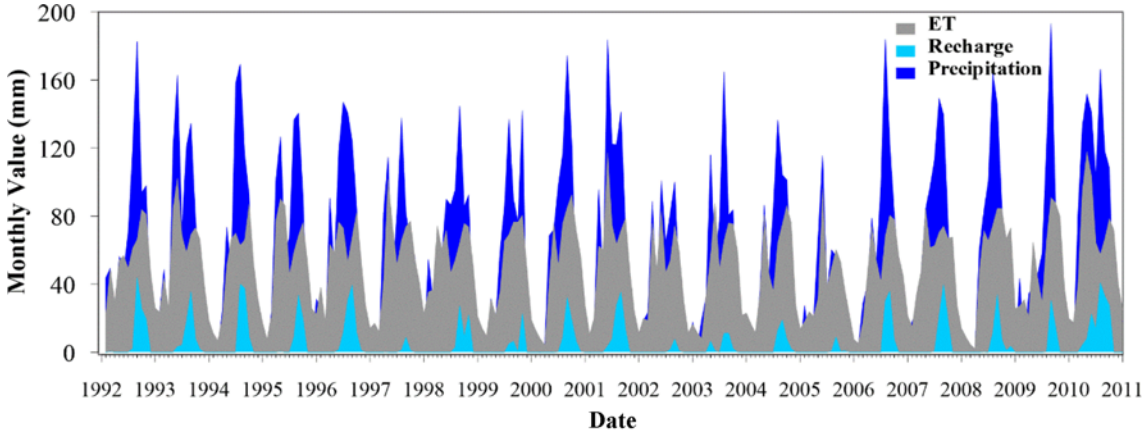

Fig. 9. Monthly Average Recharge, ET, and Surface Runoff over a Period of 1992 – 2010

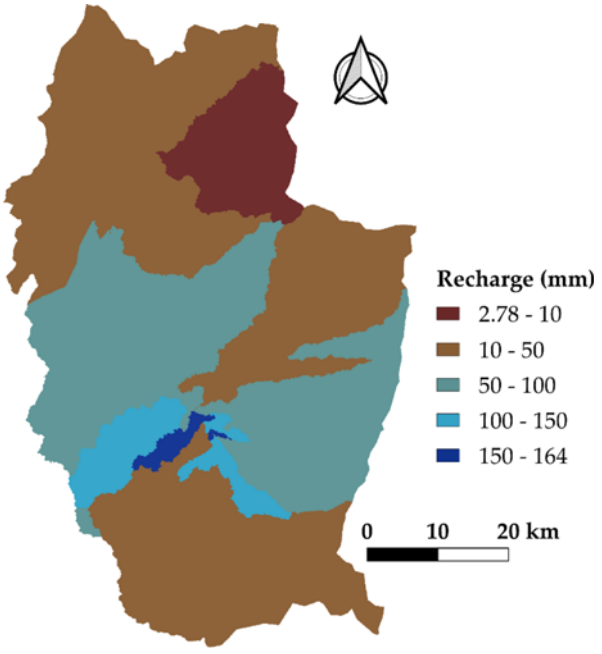

Fig. 10. Yearly Average Recharge Ranges of Katar Watershed

occurs in three months, from July – September. The long term average annual groundwater recharge is 7%. The area shows significantly high ET with a maximum monthly average value of 73 mm compared to the recharge and surface runoff. The maximum monthly average surface runoff is around 13 mm.

The longtime yearly average spatial variation of recharge is grouped into five classes (Fig. 10). The distribution shows that 50% of the area has a recharge value varying from 10 – 50 mm, which covers most of the lower elevation area of the watershed and the Kaka mountain region. A small part of the area has a high (150 – 164 mm) recharge, which is the lower mountain slope of the Southeastern and Southern highland areas.

3.2 Groundwater Potential

In GWPZ mapping using GIS-based MCDA, the determination of the weight of each layer is the most vital step, as the output chiefly depends on the apportioned weight to each thematic layer. After the thematic layers were ranked (Table 4) the pairwise matrix was constructed using the AHP plugin in QGIS and the parameters, $\lambda_{mx} = 12.015$, $CI = 0.001$, $CR = 0.001$, and normalized weight were obtained. Before giving the normalized weight, the plugin checks whether the *CR* value is less than 10%, if not it will not proceed. The ranked thematic layers and normalized weight from the AHP analysis are presented in Table 4.

WLC uses the normalized weight to combine the layers and map the GWPZs. The result was classified as low, moderate, and high GWPZs. Less than 22% of the total area has high groundwater potential, whereas more than 61% is moderate and 17% low groundwater potential.

The validation of the GWPZ was successful despite the data limitations. Wells and springs with a productivity rate of 2.6 – 100 m^3/day falls on the low GWPZ, 600 – 1,036 m^3/day on high

Table 4. Assigned Weight and Normalized Weight of Thematic Layers

Thematic layer	Assigned weight	Normalized weight (%)
Recharge	9	13.2
Geomorphology	8	11.8
LULC	7	10.3
Lithology	6	8.8
Soil	6	8.8
Slope	5	7.4
Drainage density	4	5.9
Lineament density	7	10.3
TWI	6	8.8
Curvature	4	5.9
Roughness	3	4.4
TPI	3	4.4

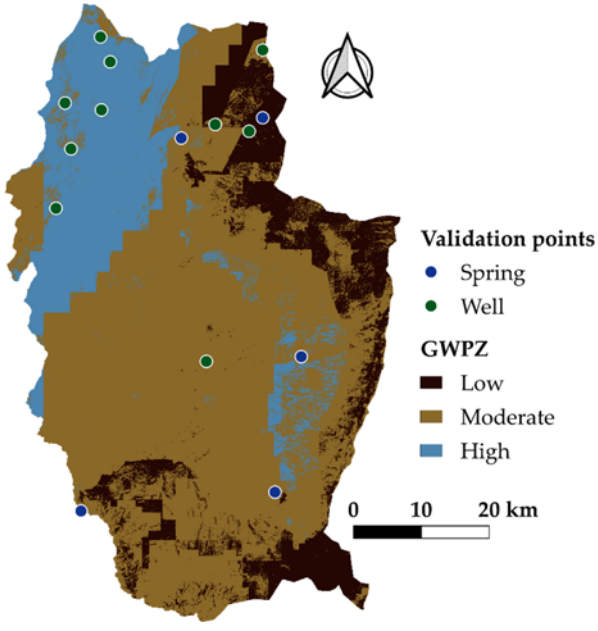

Fig. 11. Map of GWPZ and Validation Points

GWPZ and in between the two on the medium GWPZ. Fig. 11 shows the GWPZs and validation points. Mismatches were found during the validation; one well with a medium production rate falls in the high GWPZ. In general, even though the distribution of springs and wells is not uniform in the watershed the validation was successful and 93% of the production rate of the wells and springs match with the produced GWPZ map.

The large area of high GWPZ is along or northwest of the major fault lines specifically on the alluvial and lacustrine deposits (Figs. 4 and 11). This implies that the fracture system has high recharge potential or act as a linkage to recharge areas. Hence, it can be inferred that the distribution and flow of groundwater in this watershed are controlled by fracture systems, jointing, and weathering features. The Eastern area mainly along Chilalo Mountain and the high escarpment part of the watershed has poorly developed fracture systems and comprises massive

volcanic rocks and the groundwater potential is low.

The GWPZ map is not a direct reflection of the recharge map (Figs. 10 and 11). The main reason is that the WLC method is affected significantly by the scale (Malczewski, 2000); the groundwater recharge zones are not proportionate. But the two maps agree in most of the areas. The medium and high GWPZ are in the regions where the yearly average recharge is above 10 mm. In general, the groundwater recharge has a significant effect on GWPZ even though the aggregate effect of lithology and topographic attributes look dominant.

4. Conclusions

The focus of this study was recharge estimation and groundwater potential assessment using the SWAT model and GIS-based MCDA in a data-scarce region – MER. The SWAT model was calibrated and validated using SWAT-CUP and the agreement of the observed and simulated streamflow was measured using NSE, PBIAS R^2, and RSR values. As the results show the SWAT model calibration and validation are reasonably acceptable. The estimated recharge shows pronounced spatiotemporal variation. Around 50% of the area receives a yearly average recharge varying from 10 – 50 mm. The maximum recharge value in the area is 21% of the areal precipitation. The recharge, lithology, LULC, soil, and DEM-derived major water flow controlling topographic attributes were analyzed using GIS-based MCDA to map the GWPZ in a data-scarce region. The result is categorized as low, moderate, and high GWPZs. The high GWPZ covers less than 22% of the area and more than 61% of the area has moderate potential.

The assessment result was cross-validated by pumping wells and springs data in the watershed; the result shows a 93% match. However, the result should be treated wisely since most of the wells and springs, which have documented production rates are located around Ziway Lake, the validation was with a limited number of wells and springs and it was the major challenge of this study. Important results were produced in a parsimonious way using SWAT and GIS-based MCDA. The result provides valuable insight into the groundwater potential in the study area for policymakers and the community toward efficient groundwater resource management practice.

Acknowledgements

This study was funded by the Korea Ministry of Environment (MOE) as a Demand Responsive Water Supply Service Program (146515). National Meteorological Service Agency of Ethiopia (NMSAE) and the Ministry of Water Resources, Irrigation, and Electricity (MoWIE) are acknowledged for providing data.

ORCID

Bisrat Ayalew Yifru https://orcid.org/0000-0002-0593-5409
Sun Woo Chang https://orcid.org/0000-0001-9775-9475
Il-Moon Chung https://orcid.org/0000-0003-0163-7305

References

Abbaspour KC, Yang J, Maximov I, Siber R, Bogner K, Mieleitner J, Zobrist J, Srinivasan R (2007) Modelling hydrology and water quality in the pre-alpine/alpine Thur watershed using SWAT. *Journal of Hydrology* 333(2-4):413-430, DOI: 10.1016/j.jhydrol.2006.09.014

Aga AO, Chane B, Melesse A (2018) Soil erosion modelling and risk assessment in data scarce Rift Valley Lake Regions, Ethiopia. *Water* 10(11):1684, DOI: 10.3390/w10111684

Andualem TG, Demeke GG (2019) Groundwater potential assessment using GIS and remote sensing: A case study of Guna tana landscape, upper blue Nile Basin, Ethiopia. *Journal of Hydrology: Regional Studies* 24:100610, DOI: 10.1016/j.ejrh.2019.100610

Arnold JG, Allen PM, Bernhardt G (1993) A comprehensive surface-groundwater flow model. *Journal of Hydrology* 142(1-4):47-69, DOI: 10.1016/0022-1694(93)90004-S

Arnold JG, Moriasi DN, Gassman PW, Abbaspour KC, White MJ, Srinivasan R, Santhi C, Harmel RD, Van Griensven A, Van Liew MW, Kannan N, Jha MK (2012) SWAT: Model use, calibration, and validation. *Transactions of the ASABE* 55(4):1491-1508, DOI: 10.13031/2013.42256

Arnold JG, Srinivasan R, Muttiah RS, Williams JR (1998) Large area hydrologic modeling and assessment part I: Model development. *Journal of the American Water Resources Association* 34(1):73-89, DOI: 10.1111/j.1752-1688.1998.tb05961.x

Arulbalaji P, Padmalal D, Sreelash K (2019) GIS and AHP techniques based delineation of groundwater potential zones: A case study from Southern Western Ghats, India. *Scientific Reports* 9(1), DOI: 10.1038/s41598-019-38567-x

Awan UK, Ismaeel A (2014) A new technique to map groundwater recharge in irrigated areas using a SWAT model under changing climate. *Journal of Hydrology* 519:1368-1382, DOI: 10.1016/j.jhydrol.2014.08.049

Ayenew T (2007) Water management problems in the Ethiopian Rift: Challenges for development. *Journal of African Earth Sciences* 48(2-3):222-236, DOI: 10.1016/j.jafrearsci.2006.05.010

Ayenew T, Demlie M, Wohnlich S (2008a) Application of numerical modeling for groundwater flow system analysis in the Akaki catchment, Central Ethiopia. *Mathematical Geosciences* 40(8):887-906, DOI: 10.1007/s11004-008-9144-x

Ayenew T, Demlie M, Wohnlich S (2008b) Hydrogeological framework and occurrence of groundwater in the Ethiopian aquifers. *Journal of African Earth Sciences* 52(3):97-113, DOI: 10.1016/j.jafrearsci.2008.06.006

Bashe BB (2017) Groundwater potential mapping using Remote Sensing and GIS in rift valley lakes basin, Weito Sub Basin, Ethiopia. *International Journal of Scientific & Engineering Research* 8(2):43-50

Berehanu B, Ayenew T, Azagegn T (2017) Challenges of groundwater flow model calibration using MODFLOW in Ethiopia: With particular emphasis to the Upper Awash River Basin. *Journal of Geoscience and Environment Protection* 5(3):50-66, DOI: 10.4236/gep.2017.53005

Berhanu B, Melesse AM, Seleshi Y (2013) GIS-based hydrological zones and soil geo-database of Ethiopia. *Catena* 104:21-31, DOI: 10.1016/j.catena.2012.12.007

Beven KJ, Kirkby MJ (1979) A physically based, variable contributing area model of basin hydrology / Un modèle à base physique de zone d'appel variable de l'hydrologie du bassin versant. *Hydrological Sciences Bulletin* 24(1):43-69, DOI: 10.1080/02626667909491834

Calow RC, MacDonald AM, Nicol AL, Robins NS (2010) Ground water security and drought in Africa: Linking availability, access,

and demand. *Ground Water* 48(2):246-256, DOI: 10.1111/j.1745-6584.2009.00558.x

Das S (2019) Comparison among influencing factor, frequency ratio, and analytical hierarchy process techniques for groundwater potential zonation in Vaitarna basin, Maharashtra, India. *Groundwater for Sustainable Development* 8:617-629, DOI: 10.1016/j.gsd.2019.03.003

Desta H, Lemma B (2017) SWAT based hydrological assessment and characterization of Lake Ziway sub-watersheds, Ethiopia. *Journal of Hydrology: Regional Studies* 13:122-137, DOI: 10.1016/j.ejrh.2017.08.002

Drobne S, Lisec A (2009) Multi-attribute decision analysis in GIS: Weighted linear combination and ordered weighted averaging. *Informatica (Ljubljana)* 33(4):459-474

Eshtawi T, Evers M, Tischbein B (2016) Quantifying the impact of urban area expansion on groundwater recharge and surface runoff. *Hydrological Sciences Journal* 61(5):826-843, DOI: 10.1080/02626667.2014.1000916

Githui F, Selle B, Thayalakumaran T (2012) Recharge estimation using remotely sensed evapotranspiration in an irrigated catchment in southeast Australia. *Hydrological Processes* 26(9):1379-1389, DOI: 10.1002/hyp.8274

Halcrow GL, GIRDC (2008) Rift Valley Lakes Basin integrated resources development master plan study project. Phase I: Final report, Ministry of Water Resources, Addis Ababa, Ethiopia

Hussein A-A, Govindu V, Nigusse AGM (2017) Evaluation of groundwater potential using geospatial techniques. *Applied Water Science* 7(5):2447-2461, DOI: 10.1007/s13201-016-0433-0

Ibrahim-Bathis K, Ahmed SA (2016) Geospatial technology for delineating groundwater potential zones in Doddahalla watershed of Chitradurga district, India. *Egyptian Journal of Remote Sensing and Space Science* 19(2):223-234, DOI: 10.1016/j.ejrs.2016.06.002

Izady A, Davary K, Alizadeh A, Ziaei AN, Akhavan S, Alipoor A, Joodavi A, Brusseau ML (2014) Groundwater conceptualization and modeling using distributed SWAT- based recharge for the semi-arid agricultural Neishaboor plain, Iran. *Hydrogeology Journal* 23(1):47-68, DOI: 10.1007/s10040-014-1219-9

Jha MK, Chowdhury A, Chowdary VM, Peiffer S (2007) Groundwater management and development by integrated remote sensing and geographic information systems: Prospects and constraints. *Water Resour Manage* 21:427-467, DOI: 10.1007/s11269-006-9024-4

JICA (2012) The study on groundwater resources assessment in the Rift Valley Lakes Basin in the Federal Democratic Republic of Ethiopia. Final report, Japan International Cooperation, Ministry of Water & Energy, Addis Ababa, Ethiopia

Jin G, Shimizu Y, Onodera S, Saito M, Matsumori K (2015) Evaluation of drought impact on groundwater recharge rate using SWAT and Hydrus models on an agricultural island in western Japan. *Proceedings of the International Association of Hydrological Sciences* 371:143-148, DOI: 10.5194/piahs-371-143-2015

Jun C, Ban Y, Li S (2014) Open access to Earth land-cover map. *Nature* 514(7523):434-434, DOI: 10.1038/514434c

Kebede S (2013) Groundwater in Ethiopia: Features, numbers and opportunities. Springer Science & Business Media, Berlin, Heidelberg, DOI: 10.1007/978-3-642-30391-3

Kebede S, Travi Y, Asrat A, Alemayehu T, Ayenew T, Tessema Z (2008) Groundwater origin and flow along selected transects in Ethiopian rift volcanic aquifers. *Hydrogeology Journal* 16(1):55-73, DOI: 10.1007/s10040-007-0210-0

Legesse D, Ayenew T (2006) Effect of improper water and land resource utilization on the Central Main Ethiopian Rift lakes. *Quaternary International* 148(1):8-18, DOI: 10.1016/j.quaint.2005.11.003

Lerner DN, Harris B (2009) The relationship between land use and groundwater resources and quality. *Land Use Policy* 26:S265-S273, DOI: 10.1016/j.landusepol.2009.09.005

Li X, Cheng G, Lin H, Cai X, Fang M, Ge Y, Hu X, Chen M, Li W (2018) Watershed system model: The essentials to model complex human-nature system at the river basin scale. *Journal of Geophysical Research: Atmospheres* 123(6):3019-3034, DOI: 10.1002/2017JD028154

Malczewski J (2000) On the use of weighted linear combination method in GIS: Common and best practice approaches. *Transactions in GIS* 4(1):5-22, DOI: 10.1111/1467-9671.00035

Mallick J, Khan RA, Ahmed M, Alqadhi SD, Alsubih M, Falqi I, Hasan MA (2019) Modeling groundwater potential zone in a semi-arid region of Aseer using Fuzzy-AHP and Geoinformation techniques. *Water* 11(12):2656, DOI: 10.3390/w11122656

Manna F, Cherry JA, McWhorter DB, Parker BL (2016) Groundwater recharge assessment in an upland sandstone aquifer of southern California. *Journal of Hydrology* 541:787-799, DOI: 10.1016/j.jhydrol.2016.07.039

McCormack T, O'Connell Y, Daly E, Gill LW, Henry T, Perriquet M (2017) Characterisation of karst hydrogeology in Western Ireland using geophysical and hydraulic modelling techniques. *Journal of Hydrology: Regional Studies* 10:1-17, DOI: 10.1016/j.ejrh.2016.12.083

Mechal A, Birk S, Dietzel M, Leis A, Winkler G, Mogessie A, Kebede S (2017) Groundwater flow dynamics in the complex aquifer system of Gidabo River Basin (Ethiopian Rift): A multi-proxy approach. *Hydrogeology Journal* 25(2):519-538, DOI: 10.1007/s10040-016-1489-5

Mechal A, Birk S, Winkler G, Wagner T, Mogessie A (2016) Characterizing regional groundwater flow in the Ethiopian Rift: A multi-model approach applied to Gidabo River Basin. *Austrian Journal of Earth Sciences Vienna* 109:68-83, DOI: 10.17738/ajes.2016.0005

Moriasi DN, Arnold JG, Van Liew MW, Bingner RL, Harmel RD, Veith TL (2007) Model evaluation guidelines for systematic quantification of accuracy in watershed simulations. *Transactions of the ASABE* 50(3):885-900, DOI: 10.13031/2013.23153

Nair HC, Padmalal D, Joseph A, Vinod PG (2017) Delineation of groundwater potential zones in river basins using geospatial tools — An example from Southern Western Ghats, Kerala, India. *Journal of Geovisualization and Spatial Analysis* 1(1-2):5, DOI: 10.1007/s41651-017-0003-5

Pascual-Ferrer J, Pérez-Foguet A, Codony J, Raventós E, Candela L (2014) Assessment of water resources management in the Ethiopian Central Rift Valley: Environmental conservation and poverty reduction. *International Journal of Water Resources Development* 30(3):572-587, DOI: 10.1080/07900627.2013.843410

Podvezko V (2009) Application of AHP technique. *Journal of Business Economics and Management* 10(2):181-189, DOI: 10.3846/1611-1699.2009.10.181-189

Putthividhya A, Laonamsai J (2017) SWAT and MODFLOW modeling of spatio-temporal runoff and groundwater recharge distribution. Proceedings of world environmental and water resources congress 2017, May 21-25, Sacramento, CA, USA, 51-65, DOI: 10.1061/9780784480618.006

Rashid M, Lone MA, Ahmed S (2012) Integrating geospatial and ground geophysical information as guidelines for groundwater potential zones in hard rock terrains of south India. *Environmental Monitoring and Assessment* 184(8):4829-4839, DOI: 10.1007/s10661-011-2305-2

Rouholahnejad E, Abbaspour KC, Vejdani M, Srinivasan R, Schulin R, Lehmann A (2012) A parallelization framework for calibration of hydrological models. *Environmental Modelling & Software* 31:28-36, DOI: 10.1016/j.envsoft.2011.12.001

Saaty RW (1987) The analytic hierarchy process — What it is and how it is used. *Mathematical Modelling* 9(3-5):161-176, DOI: 10.1016/0270-0255(87)90473-8

Saaty TL (1990) How to make a decision: The analytic hierarchy process. *European Journal of Operational Research* 48(1):9-26, DOI: 10.1016/0377-2217(90)90057-I

Saaty TL (2008) Decision making with the analytic hierarchy process. *International Journal of Services Sciences* 1(1):83-98, DOI: 10.1504/IJSSCI.2008.017590

Singh LK, Jha MK, Chowdary VM (2018) Assessing the accuracy of GIS-based multi-criteria decision analysis approaches for mapping groundwater potential. *Ecological Indicators* 91:24-37, DOI: 10.1016/j.ecolind.2018.03.070

Sørensen R, Zinko U, Seibert J (2006) On the calculation of the topographic wetness index: Evaluation of different methods based on field observations. *Hydrology and Earth System Sciences* 10(1): 101-112, DOI: 10.5194/hess-10-101-2006

Tegegne G, Park DK, Kim Y-O (2017) Comparison of hydrological models for the assessment of water resources in a data-scarce region, the Upper Blue Nile River Basin. *Journal of Hydrology: Regional Studies* 14:49-66, DOI: 10.1016/j.ejrh.2017.10.002

Tkach RJ, Simonovic SP (1997) A new approach to multi-criteria decision making in water resources. *Journal of Geographic Information and Decision Analysis* 1(1):25-44

Weiss AD (2001) Topographic positions and landforms analysis. ESRI international user conference, July 9-13, San Diego, CA, USA

White J (1966) Convex-concave landslopes?: A geometrical study. *Ohio Journal of Science (Ohio Academy of Science)* 66(6)

Wu S, Li J, Huang GH (2008) A study on DEM-derived primary topographic attributes for hydrologic applications: Sensitivity to elevation data resolution. *Applied Geography* 28(3):210-223, DOI: 10.1016/j.apgeog.2008.02.006